Optics Communications 283 (2010) 946–950

Contents lists available at ScienceDirect

Optics Communications

journal homepage: www.elsevier.com/locate/optcom

Improve the loop frequency of liquid crystal adaptive optics by concurrent control technique

Zhaoliang Cao *, Quanquan Mu, Lifa Hu, Yonggang Liu, Li Xuan

State Key Laboratory of Applied Optics, Changchun Institute of Optics, Fine Mechanics and Physics, Chinese Academy of Sciences, Changchun, Jilin 130033, China

ARTICLE INFO

Article history:
Received 13 August 2009
Received in revised form 16 November 2009
Accepted 16 November 2009

Keywords:
Adaptive optics
Liquid-crystal wavefront correctors
Concurrent control

ABSTRACT

A method to improve the loop frequency of liquid crystal adaptive optics systems (LC AOSs) was investigated. Based on open-loop control, a concurrent control scheme was proposed and the correction frequency of the LC AOS was increased from 85 Hz to 212 Hz. A simulated correction analysis illustrates that the distortion rejection ability of our LC AOS was improved with −1.1 dB by using the concurrent control technique. A 500 m horizontal turbulence correction experiment was done to validate our considerations. Firstly, 500 m horizontal turbulence was measured and its Greenwood frequency and atmospheric coherence length is 31.5 Hz and 4–5 cm, respectively. Then, 500 m horizontal turbulence was corrected in real time by using consecutive and concurrent control methods. The corrected results indicate that the resolution and contrast of the image was significantly improved by the concurrent control method. These results show that the concurrent control method can be used for LC AOSs to improve the correction frequency.

1. Introduction

Adaptive optics systems (AOSs) have been widely applied to large-aperture telescopes to overcome the effects of atmospheric turbulence [1–4]. A wavefront corrector (WFC) is a key element of the AOS, and normally deformable mirrors (DMs) are used for this purpose. However, the finite number of actuators of DMs cannot meet the demand of telescopes with apertures of tens or even hundreds of meters [5]. To correct the atmospheric turbulence, the actuator number of the DM must be at least the approximate square of (D/r_0) [6], where, D is the aperture of the telescope, and r_0 is the atmospheric coherence length. So assume $r_0 = 20$ cm and $D = 30$ m, then the total quantity of actuators needed can be as large as 22,500. However, up to now, the maximum actuator number of the DM can be available is just 1377 [7]. Therefore, with the advantage of having millions of actuators at a reasonable cost, liquid-crystal wavefront correctors (LCWFCs) are being considered to be the candidate to surpass DMs and meet the demand of telescopes with large apertures [8–10].

Although the LCWFC has enough spatial resolution, it has a main shortcoming of a low temporal bandwidth. To improve the frame rate of the LCWFC, ferroelectric and dual frequency LC materials were used by others [11,12]. However, due to its high voltage requirement and the complexity of the control method, the dual frequency LCWFC has difficulty in handling millions of active elements. The binary phase modulation of ferroelectric LCs limits their effectiveness in WFCs. We have demonstrated that the correction of horizontal atmospheric turbulence is feasible by using nematic LCWFCs with a response speed of 270 Hz [13]. If the correction frequency can be further increased, the nematic LC AOS (NLC AOS) can be used to correct vertical atmospheric turbulence [14]. Recently Boulder Nonlinear Systems has announced the availability of the nematic liquid crystal spatial light modulator with a frame rate of as large as 500 Hz [15]. In this paper, we present a novel method to improve the correction frequency of the NLC AOS. We demonstrated that, based on a high-speed nematic LCWFC and a concurrent control technique, the correction frequency can be increased to 212 Hz.

2. Measurement of the response time of the LCWFC

Firstly, the response time of a nematic LCWFC was measured. A parallel aligned liquid crystal spatial light modulator (HSP256, BNS) is used as the LCWFC. It utilizes 256×256 pixels in a 6.14 mm × 6.14 mm area, and has a 90% zero-order diffraction efficiency. The concrete measuring method of the response time was detailed in Ref. [13]. In the experiment, the LCWFC is toggled between a 0 and 255 grey level, periodically. Two crossed polarizer were used to produce the brightness change. The first polarizer was aligned at 45°, and the second polarizer was crossed with respect to the first. The brightness change was detected by an optical power meter and the optical signal was converted to the electric signal. This electric signal was sent to an oscilloscope, and then

* Corresponding author. Tel.: +86 431 6176319; fax: +86 431 86176316.
E-mail address: caozlok@yahoo.com.cn (Z. Cao).

0030-4018/$ - see front matter © 2009 Elsevier B.V. All rights reserved.
doi:10.1016/j.optcom.2009.11.045

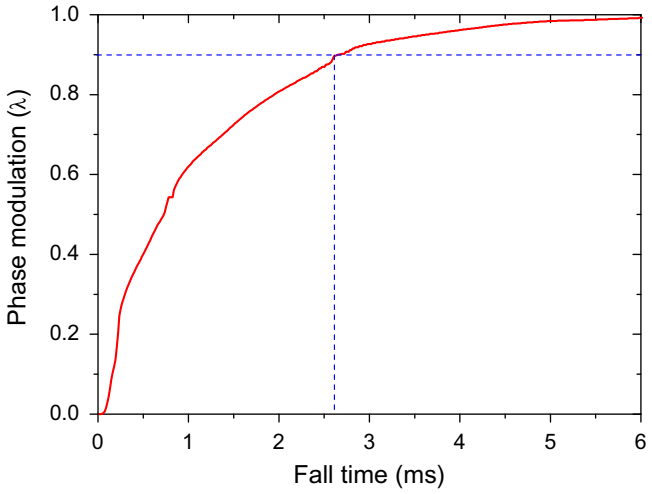

Fig. 1. Measured phase modulation as a function of fall time.

the brightness curve can be obtained. By using the measured brightness curve, the phase change of the LCWFC can be calculated. Fig. 1 illustrates the measured phase modulation as a function of the fall time. As can be seen from the figure that the phase modulation range is 1 λ (λ = 633 nm) and the phase changes rapidly at first, and then converges slowly to a constant value. Furthermore, as indicated in the figure, if a pixel response error of $\lambda/10$ can be accepted, the fall time of the LCWFC is 2.6 ms.

For a LCWFC, as demonstrated in Ref. [16], the rise time of most grey levels is littler than fall time except for few low grey levels. The effect of these low grey levels may be neglected for wavefront correction and the response time of the LCWFC may be evaluated with the fall time. We only measured the fully-off response of the LCWFC. Actually, lots of middle grey levels will be used to correct the atmospheric turbulence. In our experiment, the whole grey level range is from 0 to 255, and the minimum interval between two switching grey levels is 41. For this interval, the switch time of middle gray levels is slightly longer than the fully-switch. Therefore, we approximately use the fully-off time to represent the response time of LCWFC. According to the above approximation, we may say that the response time of LCWFC is 2.6 ms, i.e. the frame rate can be as large as 385 Hz. By using this high-speed LCWFC, it is possible to correct the slowly evolved atmospheric turbulence.

3. Improvement of loop frequency

3.1. Concurrent control scheme

The time delay of our NLC AOS was analyzed. The NLC AOS consists of a Shack-Hartmann wavefront sensor (WFS), an LCWFC and a real-time computer. The WFS has approximately 400 microlenses, an aperture of 3 mm, and a 500 Hz acquisition frequency. The real-time computer has a Core™ 2 Quad CPU (2.66 GHz), 2.0 GB memory and a Windows XP Professional operating system. A high-performance graphic card (GeForce GTX260, NVIDIA) was used to do the computation, which has 192 stream processors, 896 MB memory, and 576 MHz core clock. The time delay of each segment of the NLC AOS is shown in Fig. 2a. As the CCD camera of the WFS has a frame rate of 500 Hz, both the exposure and image output time are 2 ms. The slope matrix is calculated from the outputted Shack-Hartmann spot image; and then, the wavefront are reconstructed with modal control method. The time delay of the WFS is 4 ms. The time delay of the computation of slope matrix

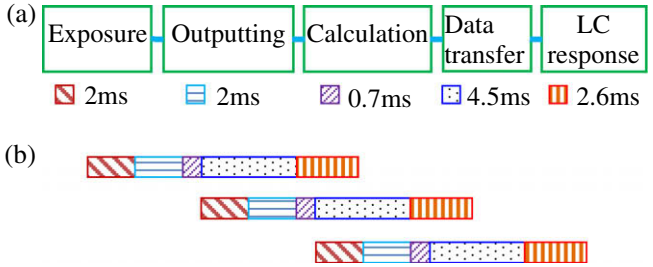

Fig. 2. Time delay segments of the NLC AOS (a) and, the concurrent control scheme (b).

and wavefront is 0.7 ms. The reconstructed wavefront needs to be sent to the LCWFC, which takes 4.5 ms. The LCWFC is driven by using the grey level picture and the response time is 2.6 ms. Thus, the total time delay from the detection of the distortion to the end of correction is 11.8 ms. We have demonstrated that open-loop control is suitable for LC AOS [17]. For open-loop operation mode [18], the adaptive system can be controlled with consecutive or concurrent mode as open-loop control is a no-feedback system. For consecutive control mode, the loop frequency of this NLC AOS is 85 Hz because of the 11.8 ms time delay. However, the loop frequency can be drastically improved by using concurrent control technique which will be illustrated as follows.

Based on open-loop control, a concurrent control scheme shown in Fig. 2b was considered. The time delay of a loop includes different segmental delays such as the WFS, calculation, data transfer, and LC response. In concurrent control shown in Fig. 2b, the next loop will be starting while the present loop has not finished yet. Therefore, the correction frequency of the LC AOS can be improved significantly. To obtain the largest correction speed, the time delay between two adjacent loops should be the longest delay segment. For our NLC AOS, the data transfer delay of 4.5 ms should be selected as the time delay of the concurrent control. Because the delay of the WFS and the calculation time is 4 ms and 0.7 ms, respectively, the next loop will be started while the present loop is still doing the calculation; this is difficult to control in the program. Thus for the convenience of the program, the end point of the calculation is selected as the start point of the next loop. With this time delay setup, the correction frequency of the NLC AOS can be increased to 212 Hz and the correction ability is therefore improved significantly.

3.2. Numerical analysis

The correction ability was analyzed for the consecutive and concurrent modes. A 5 Hz-frequency sine wave was selected as the distortion. A simulated correction was computed for the consecutive and concurrent modes and the results are shown in Fig. 3. It is shown that, although the time delay from the start of the detection to the end of the correction is 11.8 ms for both consecutive and concurrent modes, the concurrent control signal is much closer to the sine wave. Because of the faster correction frequency, the correcting amplitude of each loop of the concurrent mode is much smaller than the consecutive mode, and thus the correction signal of the concurrent mode is much closer to the distortion signal. As a result, the correction error of the concurrent mode is smaller than the consecutive mode. Fig. 4 shows the residual error of the consecutive and concurrent modes. As can be seen from the figure, the correction accuracy of the concurrent mode is much higher than the consecutive mode. The disturbance rejection can be defined in decibels as [19]

$$\mathrm{Rej(dB)} = 20\log_{10}\left(\frac{\text{output disturbance amplitude}}{\text{input disturbance amplitude}}\right). \quad (1)$$

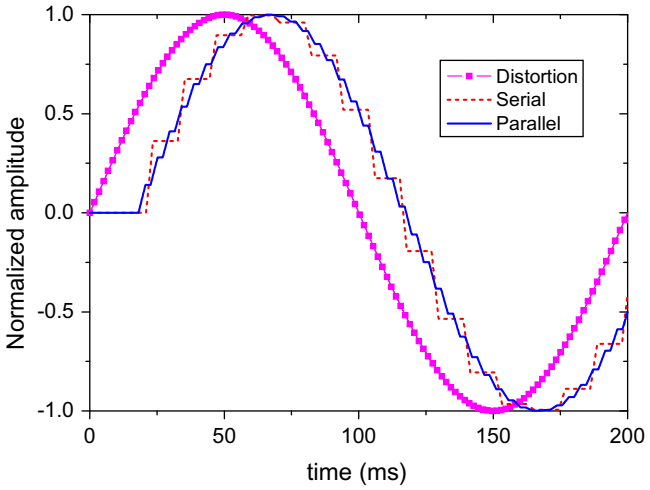

Fig. 3. Simulated correction signal of consecutive and concurrent modes for a 5 Hz sine wave distortion.

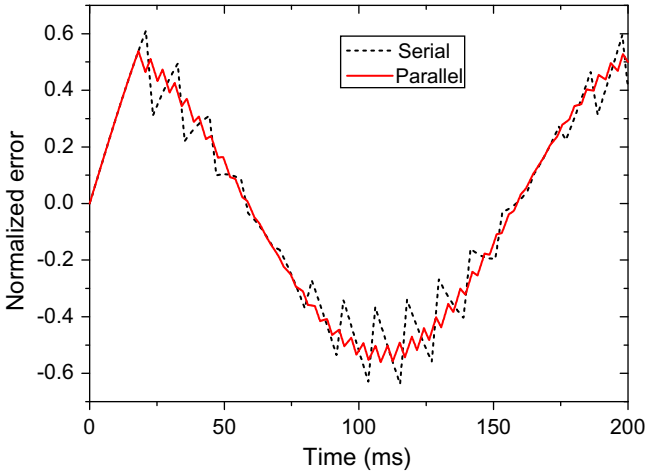

Fig. 4. Simulated corrected error of consecutive and concurrent modes.

Eq. (1) can be used to evaluate the distortion rejection ability of our NLC AOS. By using the above simulated results, the distortion rejection of consecutive and concurrent modes is −4.1 dB and −5.2 dB, respectively. Sine waves with other frequencies were also used to perform the simulated calculation and the computed results are shown in Fig. 5. As shown in Fig. 5 that, for the distortion with different frequencies, the rejection ability of the concurrent mode is always better than the consecutive mode. In addition, the average distortion rejection ability has been improved by approximately −1.1 dB. Therefore, the rejection ability of the distortional amplitude has been improved by 12%. A 500 m horizontal turbulence correction experiment was performed to verify our considerations in next section.

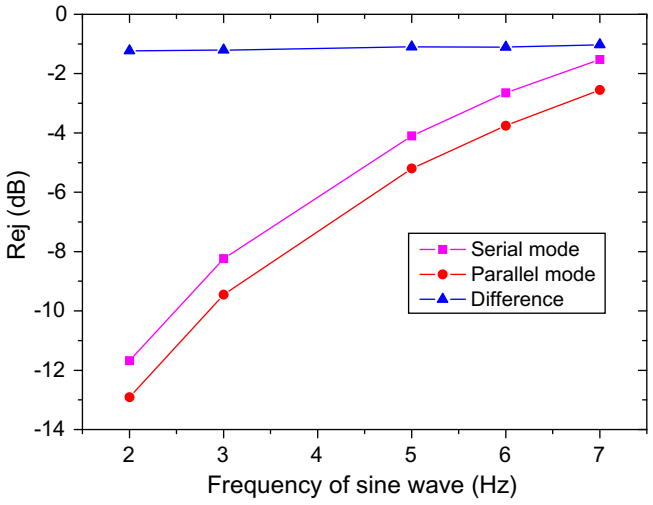

Fig. 5. Distortion rejection ability as a function of the frequency of sine wave for consecutive and concurrent modes: (■), consecutive mode, (●), concurrent mode, and (▲), the difference between the consecutive and concurrent mode.

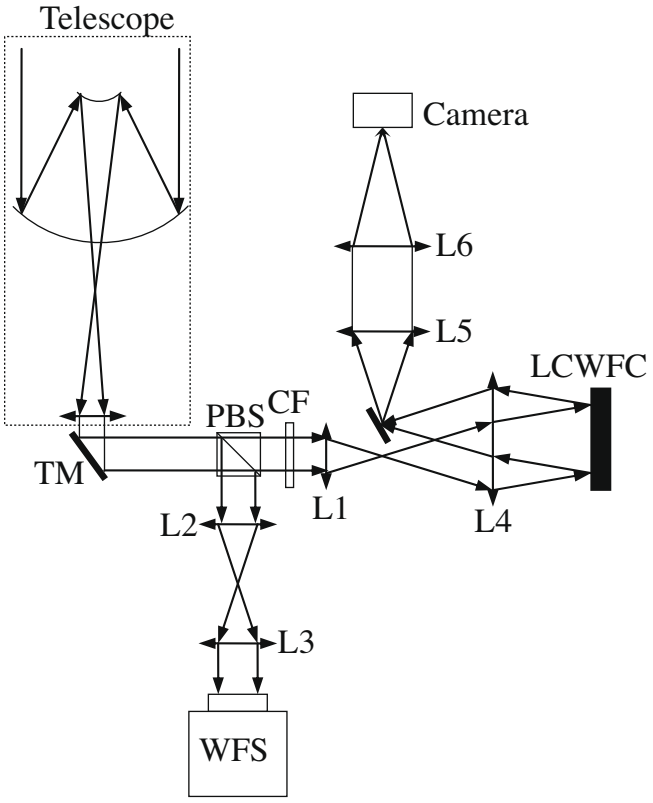

Fig. 6. Optical layout for open-loop LC AOS. TM represents tip-tilt mirror, CF represents colored filter, PBS represents polarized beam splitter and L1–L6 represents achromatic lenses.

4. Experiment

4.1. Optical layout

An optical layout was set up to measure and correct a 500 m horizontal turbulence. A fiber bundle emitting white light was used as light source. A telescope with an aperture of 400 mm was used to receive the object light. The distance between the light source and the telescope is 500 m. The NLC AOS following the telescope was used to correct the distortion due to the 500 m horizontal turbulence. The optical layout of the open-loop adaptive optics is shown in Fig. 6. The light comes out from the telescope and then is reflected by a tip-tilt mirror. The reflected beam is split into two beams by a polarized beam splitter (PBS). The reflected beam is used to measure the distortions. The other beam is filtered by a narrowband colored filter working at the wavelength of 633 nm. This filtered light is then corrected by the LCWFC and goes to a camera.

4.2. Measurement of horizontal turbulence

By using above optical setup, the Greenwood frequency of 500 m horizontal turbulence was measured firstly. The altitude of the experimental area is 200 m. At the afternoon of the 20th of March, 2009, the phase change as a function of the time was measured by using a Shack-Hartmann WFS. The measuring time of each wavefront was 2 s and 10 thousands of wavefronts were measured and saved. For each wavefront, 20 phase points were selected to do the calculation. For each phase point, the phase change function was converted to the frequency domain by using Fourier transform. Then, an averaged spectrum was acquired from 20 spectral curves. At last, the averaged spectrum was integrated and shown in Fig. 7 to illustrate the relation between the residual wavefront variance and the control bandwidth. The higher-order wavefront variance (tilt removed) due to finite control bandwidth can be expressed as [20]

$$\sigma^2 = \left(\frac{f_G}{f_{3dB}}\right)^{5/3}, \quad (2)$$

where f_G and f_{3dB} is Greenwood frequency and 3 dB cutoff frequency, respectively. According to Eq. (2), if $f_G = f_{3dB}$, the wavefront variance is 1 rad^2. Generally, if the residual wavefront variance is smaller than 1 rad^2, the atmospheric turbulence has little need to be corrected [6]. Therefore, we measure and calculate the Greenwood frequency under the condition of $\sigma^2 = 1$ rad^2. Similarly, according to Eq. (2), the Greenwood frequency can also be calculated by using $f_G = f_{3dB}/4$ under the condition of $\sigma^2 = 0.1$ rad^2. According to Fig. 7, the control bandwidth f_{3dB} is 162 Hz while $\sigma^2 = 0.1$ rad^2. Therefore, the Greenwood frequency f_G is calculated to be 31.5 Hz.

The atmospheric coherence length r_0 was also measured for 500 m horizontal turbulence. Differential motion method was selected to perform the r_0 measurement [21]. The r_0 can be measured according to the variance of the relative distance between two separated images

$$\sigma_{xy}^2 = F^2\lambda^2 r_0^{-5/3}[0.697D^{-1/3} - 0.484d^{1/3}], \quad (3)$$

where σ is the variance of image motion, F is the focal length of the telescope, λ is the wavelength, D represents the diameter of sub-aperture, and d is the separation distance. The concrete measuring optical layout is shown in Fig. 8. Two lenses with apertures of $D = 30$ mm were used to obtain two images. The distance $d = 600$ mm, $\lambda = 633$ nm and focal length of the lens $F = 250$ mm. The

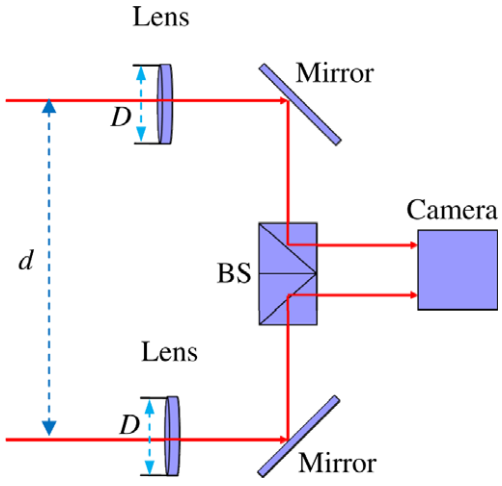

Fig. 8. Optical setup for the measurement of atmospheric coherence length, BS is the beam splitter.

r_0 of horizontal turbulence was measured from 10:30 am, March 18th, 2009 to 8:30 am, March 19th with an interval of 30 min. The r_0 as a function of the time is shown in Fig. 9. It indicates that the r_0 of horizontal turbulence changes drastically from day to night. In the day, the value of r_0 is only 4 cm; but it can be up to 24 cm at night.

4.3. Adaptive correction with consecutive and concurrent mode

A 500 m horizontal turbulence correction experiment was done with the consecutive and concurrent loop control method to validate our considerations. At the afternoon of the 20th of March, 2009, the adaptive correction experiment was done after the Greenwood frequency was measured. The measured Greenwood frequency of 500 m horizontal turbulence was 31.5 Hz. The r_0 of 500 m horizontal turbulence was measured to be about 4–5 cm at that afternoon. Before the correction, the image of the fiber bundle was blurry, as shown in Fig. 10a. Firstly, the consecutive correction mode was used to perform the adaptive correction with a 85 Hz correction frequency. The corrected image is shown in Fig. 10b and indicates that the core of each fiber cannot be clearly resolved. However, when the concurrent mode with a 212 Hz correction frequency was used to perform the adaptive correction, the

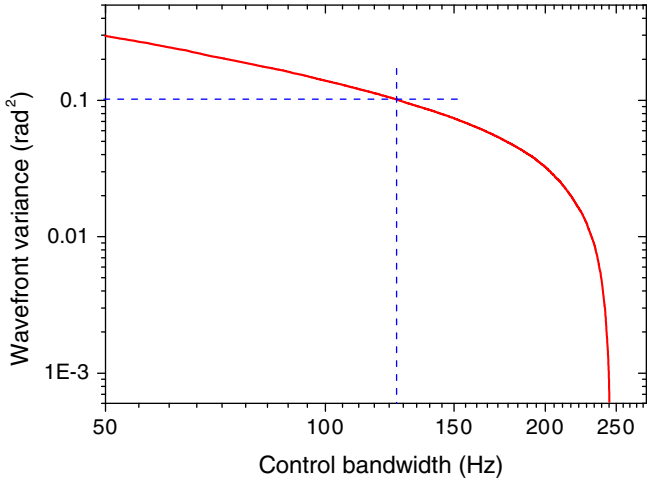

Fig. 7. Residual wavefront variance as a function of control bandwidth for 500 m horizontal turbulence.

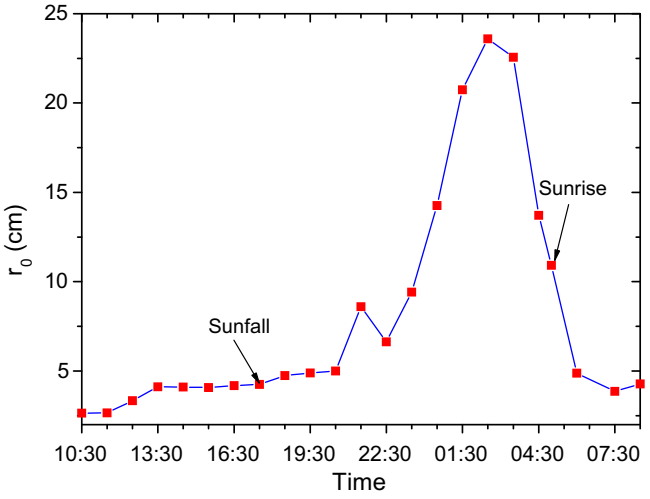

Fig. 9. Measured atmospheric coherence length as a function of time.

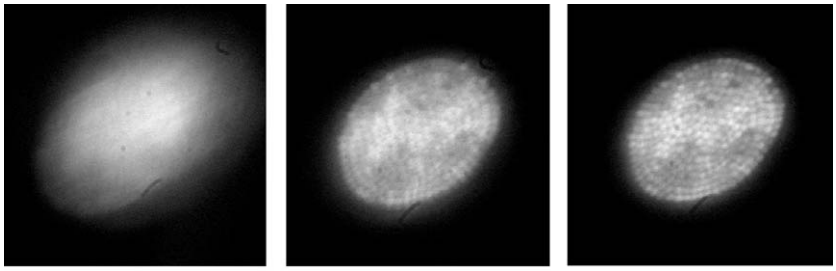

Fig. 10. Images of fiber bundle: (a) without correction; (b) corrected with consecutive mode; (c) corrected with concurrent mode.

corrected image as shown in Fig. 10c clearly shows that the fiber core was resolved. This fiber core has a field angle of 0.41″ relative to the telescope. Considering the diffraction-limited angular resolution of the telescope is 0.4″ at the wavelength of 633 nm, we can say the optical system has obtained diffraction-limited resolution after the concurrent control. Compared with the consecutive correction, the resolution and contrast of the corrected image were significantly improved. Consequently, we can conclude that, based on open-loop control, the concurrent control technique can be used to increase the correction frequency of LC AOSs and therefore to improve the distortion rejection ability. This concurrent control method can be used by all LC AOSs that operate in the open-loop control.

5. Conclusions

In summary, we have demonstrated that, based on open-loop control, LC AOSs can be operated with a concurrent control mode and the correction frequency can be improved significantly. Firstly, an LCWFC with a switching frequency of 385 Hz was presented; the loop frequency of the NLC AOS can be increased to 85 Hz. Subsequently, based on open-loop control, a concurrent control scheme was considered to improve the correction frequency of the LC AOS. By using this method, the correction frequency can be increased to 212 Hz. Distortion rejection ability is increased by −1.1 dB. Finally, a 500 m horizontal turbulence correction experiment was done to validate our considerations. Compared with the consecutive mode, the resolution and contrast of the image was significantly improved with the concurrent control. The results indicate that this concurrent control method is effective and can be used for LC AOSs to improve the correction ability. This is particularly helpful to the NLC AOSs due to their slower loop frequency.

Acknowledgements

This work is supported by the National Natural Science Foundation of China with Grant Numbers of 60736042, 60578035 and 50703039.

References

[1] M. Schöck, D.L. Mignant, G.A. Chanan, et al., Proc. SPIE 4839 (2003) 813.
[2] P.T. Ryan, S. Milster, J.D. Drummond, Proc. SPIE 4860 (2003) 311.
[3] A. Piterman, Z. Ninkov, B.S. Backer, et al., Proc. SPIE 3353 (1998) 447.
[4] F. Roddier, Appl. Opt. 27 (1998) 1223.
[5] B.L. Ellerbroek, C. Boyer, C. Bradley, et al., Proc. SPIE 6272 (2006) 62720D-1.
[6] F. Roddier, Adaptive Optics in Astronomy, Cambridge University Press, 1999, pp. 13–15.
[7] <http://www.adaptiveoptics.org/News_1207_2.html>.
[8] L. Hu, L. Xuan, Y. Liu, et al., Opt. Express 12 (2004) 6403.
[9] G.D. Love, Appl. Opt. 36 (1997) 1517.
[10] M.A.A. Neil, M.J. Booth, T. Wilson, Opt. Lett. 23 (1998) 1849.
[11] D.C. Burns, I. Underwood, J. Gourlay, et al., Opt. Commun. 119 (1995) 623.
[12] S.R. Restaino, D. Dayton, S. Browne, et al., Opt. Express 6 (2000) 2.
[13] Z. Cao, Q. Mu, L. Hu, et al., Opt. Express 16 (2008) 7006.
[14] Z. Cao, Q. Mu, L. Hu, et al., Opt. Express 17 (2009) 2530.
[15] <http://www.bnonlinear.com/>.
[16] H. Wang, T.X. Wu, X. Zhu, et al., J. Appl. Phys. 95 (2004) 5502.
[17] Q. Mu, Z. Cao, L. Hu, et al., Appl. Opt. 47 (2008) 4297.
[18] K.M. Morzinski, K.B.W. Harpsœe, D.T. Gavel, et al., Proc. SPIE 6467 (2007) 64670G-1.
[19] D. Dayton, S. Browne, J. Gonglewski, et al., Appl. Opt. 40 (2001) 2345.
[20] R.K. Tyson, Principles of Adaptive Optics, second ed., Academic Press, 1998, p. 73.
[21] A.C. Slavin, A.L. Wells, R.Q. Fugate, et al., Proc. SPIE 3125 (1997) 241.